

Current Distribution in Shielded Cable-Connector Systems for Power Transmission in Electric Vehicles

Stephan Frei, Abid Mushtaq, Katharina Hermes, Robert Nowak
On-board System Lab
TU Dortmund University
Dortmund, Germany
stephan.frei@tu-dortmund.de

Abstract—With the electrification of vehicle propulsion systems, shielded cables were introduced for delivering the power from HV-battery to inverter and/or from inverter to three-phase motor. On the one hand the shield should improve EMC behaviour, on the other hand the shield should protect passengers and service staff from the high voltage. While in typical communication application of shielded cables the shield carries the return current from the inner conductor and the current sum is zero, the automotive power cable employs a second shielded, and, for three phase applications, a third shielded cable, for the return currents. There is no current injection into the shield. Shield currents are mainly induced by inductive coupling. Knowing the shield currents is essential for evaluating the common mode current and thus the relevant fields caused by a cable configuration. In this paper an analytic approach for estimating the current distribution in and the fields from a shielded cable system for EV for low frequencies is presented. With this method typical systems are calculated and discussed regarding the common mode currents and the magnetic fields.

Keywords—shielded cables; power electronics; EMC; automotive; electric vehicles

I. INTRODUCTION

Shielded cables are commonly used in electric vehicles (EV) for delivering the power from high voltage (HV)-battery to inverter and/or from inverter to three-phase motor (Fig. 1). Safety demands and the high RF currents require usage of a shield. In communication applications of shielded cables, the shield carries the return current from the inner conductor and the current sum should be zero. The automotive power cable employs a second shielded, and, for three phase applications, a third shielded cable, for the return currents. There is no injected shield current. The shield currents are mainly induced by inductive coupling and are not forced to be identical with the currents through the inner conductors of the shielded cables. The mutual coupling between the different conductors must be taken into account. Furthermore, connectors can affect significantly the shield currents. Knowing the shield currents is essential for evaluating the common mode currents and this way the relevant electric and magnetic fields, caused by a power cable system.

While the electromagnetic fields from vehicle systems are mainly measured according to CISPR 25 [1], magnetic fields for health protection are limited by ICNIRP-recommendations [2]. In the first case the E-fields up to 30 MHz are most interesting. In the second case, the magnetic fields generated by uncompensated currents must be known.

Different investigations have analysed shielded cables for EV, e.g. [3]. Mainly the transfer impedance and the termination impedance were considered in the past. The multi-conductor transmission line structure (MTL) and the special excitation modes were not analysed. In [4] HV cables are treated as MTL. The computation approach is similar to the one shown here.

The basic theory for shielded cables was developed by Schelkunoff [5]. He introduced the surface and transfer impedance of a cable shield as the per unit length impedance a shield current must be multiplied with, in order to get the longitudinal electric field on the shield surface nearest to the return path and the longitudinal electric field on the adjacent surface. He did not consider coupled shielded cables. In [6] coupling between shielded cables over a ground plane was analyzed and discussed. Here the transfer impedance is not considered. In [7] and [8] a full model based on multi-conductor transmission line theory (MTL) was considered. The mentioned papers have in common that mainly immunity against disturbances is subject of analysis, and the coupled termination voltage was analyzed, when the shield carries the return current from the inner conductor. The radiation from coaxial cables was analyzed e.g. in [9]. Here a single coaxial cable driven in differential mode. It could be shown that the external loop current is responsible for the antenna field.

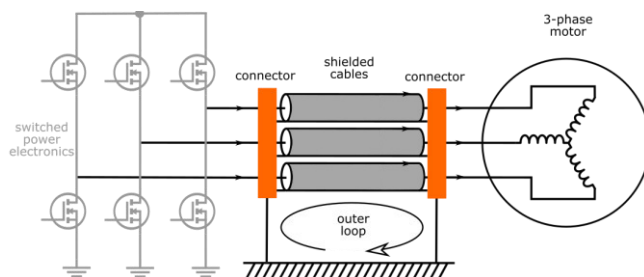


Fig. 1. Power electronic system for vehicle propulsion.

As the currents in EV-cable shields are not impressed currents and not identical to the inner conductor currents the given approaches must be extended. In this paper an analytic approach for estimating the currents in a multi-conductor shielded cable connector systems over a perfectly conducting ground plane is presented. Two items are assumed to be relevant:

1. The field emissions from the EV cables are considered to be based on the leakage current (radiating antenna current), i.e. the sum current on cable shield and inner conductor [6].

2. The longitudinal electric fields from shield current along the cable outside of the shield, the outer loop (Fig. 1), affecting electric antennas.

In both cases, the connectors have to be considered, adding an additional voltage drop and influencing the shield currents.

After presenting the method, typical systems are calculated and discussed regarding the currents and fields. A two-cable configuration is analyzed that can be easily extended to a three-cable configuration. The transfer admittance and the dielectric conductor losses are assumed to be small and were not considered. This paper does not provide direct computations of radiated fields in EV. It points out the general mechanisms, responsible for field emissions from shielded cable connector systems.

II. CALCULATION MODEL FOR SHIELDED CABLES

A. Equivalent Circuit for Shielded Cables and Calculation Approach

A basic vehicle power cable configuration made of shielded HV-cables can be modeled as shown in Fig. 2. A cross section of the cables is given in Fig. 3. This could be a connection from HV-battery to DC/DC or DC/AC converter. The stimulating terminations are modeled as uncoupled Thevenin sources. All terminations are modeled as simple impedances. Shield currents can only be generated by mutual coupling.

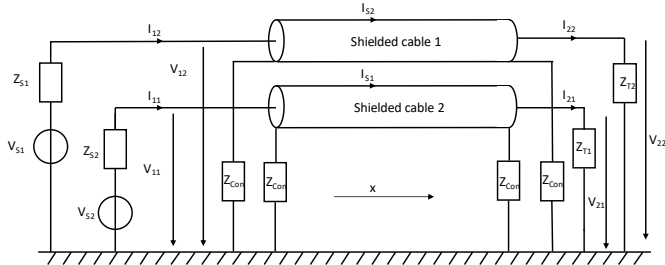


Fig. 2. Circuit diagram of a shielded cable configuration over ground that can be driven in DM and CM. This configuration is investigated.

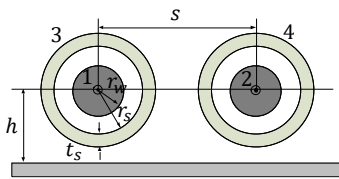


Fig. 3. Cross section of the shielded cable configuration with conductor indices.

The following analysis is based on [7] (applied also in e.g. [10]). Here only the basic concept is summarized. Furthermore, it is assumed here that all currents return through the ground plane.

In general, the transmission line theory has difficulties to handle the radial current distributions that must be considered for shielding structures. The following points must be taken into account:

1. In the configuration according to Fig. 2, there is no injected current in the cable shield. A current can flow in

the shield only due to the induced voltage from the alternating magnetic flux in the loop area between shield and ground. With increasing frequency, the current rises and will compensate the magnetic flux in the loop. Finally, the flux will be zero, when there are no additional impedances, equilibrium is reached. In a balanced system the current in the shield will be the same as the current in the inner conductor. The current from mutual induction in the shield is shaped by the magnetic flux from the shield and the inner conductor. At the outer side of shield the magnetic flux is strongly reduced with rising frequency. I.e., the current density approaches zero. Towards the center of the conductor it increases with maximum on the inner shield wall.

2. The impedances of shielded cables are dominated by skin effect. For thin solid shields, skin effect approximations can be used for inner and outer surfaces. Analytical approaches are available for pure triaxial configurations.
3. **Transfer impedance is not required for calculation of the currents in the conductors.** Only when voltage drop on outer surface must be known, transfer impedance is needed. It considers the outer voltage drop in a shielded cable, where the shield current is opposite to the inner conductor current and the outside of the shielded cable is free from magnetic fields.

Different cut off frequencies can be defined. Typical electric vehicle HV-cable configurations show the following three dedicated frequencies:

f_{cISC} : Around 1 kHz – 10 kHz mutual inductance generates a shield current in the same order of magnitude as the current in the inner conductor.

f_{cSE} : Around 50 kHz skin effect becomes visible in shields with typical thickness in submillimeter range.

f_{cTI} : Around 500 kHz shield transfer impedance is not dominated by DC value any more, current densities on inner and outer shield walls are significantly different.

For further calculation the currents through the cables with numbers 1 and 2 are given by the vector \mathbf{I} where I_1 denotes a current through the inner conductor and I_S denotes a current through the shield. \mathbf{V} is the vector with the voltage drops along the cables:

$$\mathbf{I} = \begin{bmatrix} I_{I_1} \\ I_{I_2} \\ I_{S_1} \\ I_{S_2} \end{bmatrix}; \quad \mathbf{V} = \begin{bmatrix} V_{I_1} \\ V_{I_2} \\ V_{S_1} \\ V_{S_2} \end{bmatrix}$$

The longitudinal voltage drop $\dot{\mathbf{V}} = d\mathbf{V}/dx$ is given by

$$\dot{\mathbf{V}}(x) = -(\mathbf{Z}'_C + j\omega\mathbf{L}'_{ext.})\mathbf{I}(x). \quad (1)$$

The inner impedance \mathbf{Z}'_C of the shielded cable is:

$$\mathbf{Z}'_C = \begin{bmatrix} Z'_I & 0 & 0 & 0 \\ 0 & Z'_I & 0 & 0 \\ 0 & 0 & Z'_S & 0 \\ 0 & 0 & 0 & Z'_S \end{bmatrix}. \quad (2)$$

Here Z'_I is the impedance of the inner conductor of the shielded cable and Z'_S denotes the shield impedance. Skin effect and internal inductance should be considered here.

The external inductance matrix \mathbf{L}'_{ext} can be simplified, if symmetry is assumed with two equal cables at same height to

$$\mathbf{L}'_{\text{ext}} = \begin{bmatrix} L'_I & L'_M & L'_S & L'_M \\ L'_M & L'_I & L'_M & L'_S \\ L'_S & L'_M & L'_S & L'_M \\ L'_M & L'_S & L'_M & L'_S \end{bmatrix}. \quad (3)$$

With L'_I and L'_S are the self-inductances of the inner conductors and shields. L'_M is the mutual coupling inductance. $j\omega\mathbf{L}'_{\text{ext}}$ dominates the impedance \mathbf{Z}'_C at higher frequencies.

The capacitance matrix considering the same symmetry can be written as

$$\mathbf{C}'_C = \begin{bmatrix} C'_{IS} & 0 & -C'_{IS} & 0 \\ 0 & C'_{IS} & 0 & -C'_{IS} \\ -C'_{IS} & 0 & C'_{IS} + C'_{SS} + C'_{S0} & C'_{SS} \\ 0 & -C'_{IS} & C'_{SS} & C'_{IS} + C'_{SS} + C'_{S0} \end{bmatrix}. \quad (4)$$

Here C'_{IS} is the capacitance between inner conductor and shield. C'_{SS} is the capacitance between the shields and C'_{S0} is the capacitance between shield and ground plane.

The current change $\dot{\mathbf{I}} = d\mathbf{I}/dx$ is given by

$$\dot{\mathbf{I}}(x) = -j\omega\mathbf{C}'_C \mathbf{V}(x). \quad (5)$$

As mentioned above, isolation currents can be assumed to be small and were not considered, i.e. $\mathbf{G} = \mathbf{0}$.

B. Cable Parameters

A solid wire approximation for the impedance of an inner conductor with conductivity σ and radius r_i , neglecting proximity effect, gives for

$$Z'_I = \frac{jk}{2\pi r_i \sigma} \frac{J_0(jkr_i)}{J_1(jkr_i)}. \quad (6)$$

With $k = \sqrt{j\omega\mu\sigma}$, J_0 and J_1 are the Bessel functions of first kind and zeroth/first order. For the shield a thin sheet approach can be used:

$$Z'_S = \frac{k}{2\pi r_s \sigma} \coth(kt_s). \quad (7)$$

With r_s is the radius of the shield and t_s is the thickness.

For the symmetrical case with identical cables the cable parameters L'_I , L'_S and L'_M can be computed using the following formulas:

$$L'_I = c \ln\left(\frac{2h}{r_i}\right), \quad (8)$$

$$L'_S = c \ln\left(\frac{2h}{r_s + t_s}\right),$$

$$L'_M = \frac{c}{2} \ln\left(1 + \frac{4h^2}{s^2}\right).$$

With $c = \mu_0/(2\pi)$. h and s can be found in Fig. 3.

The capacitance parameters C'_{IS} , C'_{SS} , and C'_{S0} can be found using the following relations:

$$\begin{bmatrix} C'_{S0} + C'_{SS} & -C'_{SS} \\ -C'_{SS} & C'_{S0} + C'_{SS} \end{bmatrix} = \mu_0 \epsilon_0 \begin{bmatrix} L'_S & L'_M \\ L'_M & L'_S \end{bmatrix}^{-1}, \quad (9)$$

$$C'_{IS} = \frac{2\pi\epsilon}{\ln\left(\frac{r_s}{r_i}\right)}.$$

C. Transfer Impedance

The transfer impedance Z'_T will give the outer shield voltage drop, when the same current in opposite direction flows through the shield as the inner conductor current, and the outer space is free from magnetic fields. The transfer impedance of a cable with thickness t_s can be computed e.g. with Demoulin's formula:

$$Z'_T = \frac{k}{2\pi r_a \sigma \sinh(kt_s)} + K\sqrt{\omega}e^{+j\frac{\pi}{4}} + j\omega(L_H - L_B) \quad (10)$$

For a typical automotive HV-copper-cable from the cable manufacturer Coroplast with inner conductor cross section of 35 mm^2 , $r_a = 5.7 \text{ mm}$, $L_H = 3.65 \text{ nH}$, $L_B = 3.78 \text{ nH}$, $K = 0.5 \cdot 10^{-7}$, $R_0 = 3.3 \text{ m}\Omega$, and $t_s = 0.2 \text{ mm}$ the transfer impedance over frequency is shown in Fig. 4.

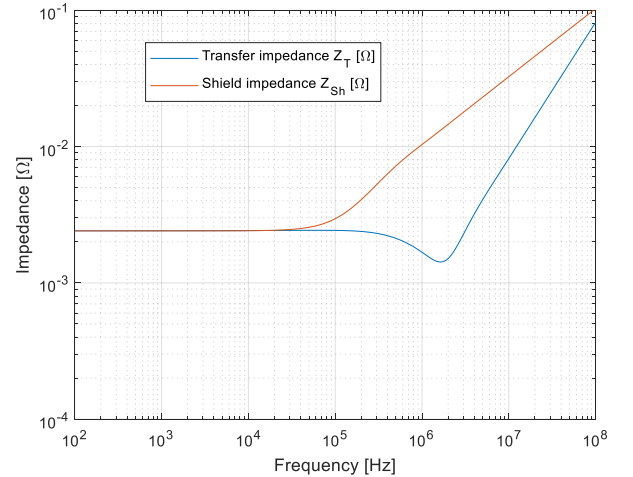


Fig. 4. Transfer impedance and shield impedance of a 35 mm^2 Coroplast automotive cable calculated with Demoulin's formula and the thin shield approach.

D. Connectors

Connectors, as shown in Fig. 5, with two and three poles and shield for HV-applications can be modeled as equivalent circuits considering the important properties like

- connector resistance,

- self and mutual inductance, and
- self and mutual capacitance.

Mainly the connector contact resistance and the stray inductance from missing symmetry, that is not compensated [11], influences the behavior. Thus, connectors here are modeled as an resistor with 1 mΩ and a serial inductance with 2 nH as stray inductance (Fig. 6). Measurements have shown that the critical shield resistance of typical HV-connectors degrades after several connection/disconnection cycles. It quickly rises up to 10 mΩ and more. Coupling is assumed to be weaker than in the cables and is not considered here.

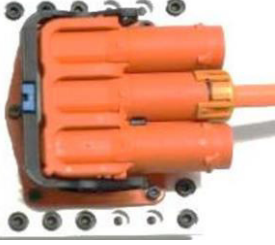


Fig. 5. Typical HV-connector.

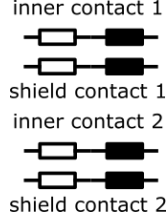


Fig. 6. Equivalent circuit for HV-connector.

When no other values are given $Z_{\text{Con}}=1 \text{ m}\Omega+j\omega 2 \text{ nH}$.

III. CALCULATION OF CURRENTS AND VOLTAGES

As shown in Fig. 2, there are Thevenin sources assumed for feeding the inner conductors. This way vectors for source voltages \mathbf{V}_S at the beginning and source voltages at the load side \mathbf{V}_L can be defined. The same can be done with impedances. As the connector impedances for the inner conductors are assumed to be much smaller than the termination impedances, the values are neglected here. The following vectors and matrices can be formulated according to Fig. 2:

$$\mathbf{V}_S = \begin{bmatrix} V_{S_1} \\ V_{S_2} \\ 0 \\ 0 \end{bmatrix}, \mathbf{V}_L = \begin{bmatrix} 0 \\ 0 \\ 0 \\ 0 \end{bmatrix}, \mathbf{Z}_S = \begin{bmatrix} Z_{S_1} & 0 & 0 & 0 \\ 0 & Z_{S_2} & 0 & 0 \\ 0 & 0 & Z_{\text{Con}} & 0 \\ 0 & 0 & 0 & Z_{\text{Con}} \end{bmatrix}, \quad (11)$$

$$\mathbf{Z}_L = \begin{bmatrix} Z_{T_1} & 0 & 0 & 0 \\ 0 & Z_{T_2} & 0 & 0 \\ 0 & 0 & Z_{\text{Con}} & 0 \\ 0 & 0 & 0 & Z_{\text{Con}} \end{bmatrix}.$$

With the transformation matrix \mathbf{T} for diagonalization of the product \mathbf{YZ} from $\mathbf{Z} = \mathbf{Z}'_C + j\omega\mathbf{L}'_{\text{ext}}$ and $\mathbf{Y} = j\omega\mathbf{C}'_C$, l is the length of the cable, \mathbf{Y}^2 the eigenvalue matrix, $\mathbf{Z}_0 = \mathbf{Y}^{-1}\mathbf{T}\mathbf{Y}\mathbf{T}^{-1} = \mathbf{Y}_0^{-1}$, a chain parameter matrix Φ can be calculated as described in detail in [12]:

$$\Phi_{11} = \frac{1}{2}\mathbf{Y}^{-1}\mathbf{T}(e^{\gamma l} + e^{-\gamma l})\mathbf{T}^{-1}\mathbf{Y},$$

$$\Phi_{12} = -\frac{1}{2}\mathbf{Z}_0(\mathbf{T}(e^{\gamma l} - e^{-\gamma l})\mathbf{T}^{-1}),$$

$$\Phi_{21} = -\frac{1}{2}(\mathbf{T}(e^{\gamma l} - e^{-\gamma l})\mathbf{T}^{-1})\mathbf{Y}_0,$$

$$\Phi_{22} = \frac{1}{2}\mathbf{T}(e^{\gamma l} + e^{-\gamma l})\mathbf{T}^{-1}.$$

Current and voltage vectors for beginning, denoted with 1, and the end of the cable, denoted with 2, can finally be calculated as:

$$\mathbf{I}_1 = (\Phi_{12} - \Phi_{11}\mathbf{Z}_S - \mathbf{Z}_L\Phi_{22} + \mathbf{Z}_L\Phi_{21}\mathbf{Z}_S) \cdot (\mathbf{V}_L - (\Phi_{11} - \mathbf{Z}_L\Phi_{21})\mathbf{V}_S),$$

$$\mathbf{I}_2 = \Phi_{21}\mathbf{V}_S + (\Phi_{22} - \Phi_{21}\mathbf{Z}_S)\mathbf{I}_1, \quad (12)$$

$$\mathbf{V}_1 = \mathbf{V}_S - \mathbf{Z}_S\mathbf{I}_1,$$

$$\mathbf{V}_2 = \mathbf{V}_L - \mathbf{Z}_L\mathbf{I}_2.$$

IV. APPLICATION TO EV-SHIELDED CABLE CONFIGURATIONS

A. General Approach

For investigation of shielding performance different properties can be calculated. As discussed above the normalized leakage current used e.g. in [6] can be expressive. It can be defined as:

$$I_{\text{Leak}} = (I_1 - I_S)/I_1 \quad (13)$$

The leakage current shows, similar to the CM-current, the lack of compensation and how large a magnetic field might become. Adding both leakage currents, a CM-current for the whole system can be defined. Furthermore, as discussed already above, the longitudinal electric field E_L on the external shield is an important property, how electric antennas like the 1 m-rod in CISPR-25 or a vehicle antenna for AM radio reception will be affected. It depends on the shield current I_S and the transfer impedance of a cable Z'_T ,

$$E_L = I_S Z'_T. \quad (14)$$

The positions of the cables are investigated as well. A compact and a large distance configuration is investigated. Important parameters are summarized in Table 1 according to Fig. 3.

Table 1: Properties of investigated cable (Coroplast 35 mm²)

Property	Value
Radius of inner conductor r_w	3.34 mm
Radius of shield r_s	7.7 mm
Thickness of shield t_s	0.2 mm
ϵ_r of dielectrics	3 (estimation)
Length of cable l	1.5 m
Thickness of isolation t_{iso}	1 mm
Distance between shielded cables s (compact large dist.)	$2(r_s + t_s + t_{\text{iso}})$ 2.5 cm
Distance above plate h (compact large distance)	$(r_s + t_s + t_{\text{iso}})$ 5 cm

The power electronic devices generate CM and DM disturbances. As the special disturbance behavior of a power electronic system is not subject of this paper, a general pure CM and pure DM excitation was investigated in most cases. In CM $V_{S_1} = V_{S_2}$, in DM $V_{S_1} = -V_{S_2}$. The source impedances Z_{S_1} and Z_{S_2} were chosen to be very large in order to reproduce the behavior of an ideal current source.

As the currents in EV-shields are not impressed but generated by induction depending on the frequency and other parameters, an analysis is required.

B. Analysis of Geometry

In Fig. 7 the normalized currents for CM and DM excitation are shown for the two geometry sets. The parameters are given in Table 1 according to Fig. 3.

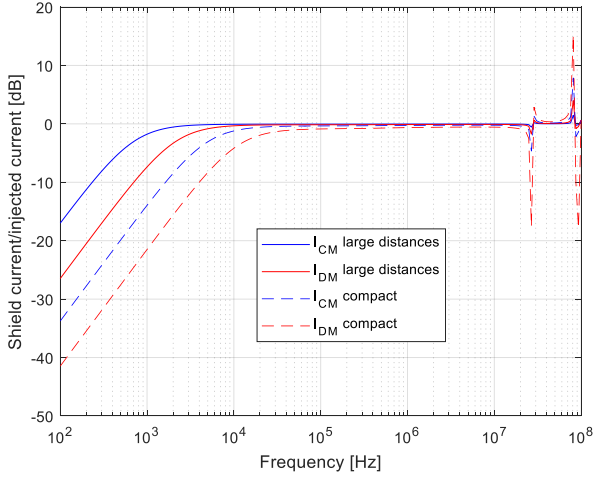


Fig. 7. Shield current, normalized to current of inner conductor, for CM and DM excitation for different distances between the cables and the cables to ground.

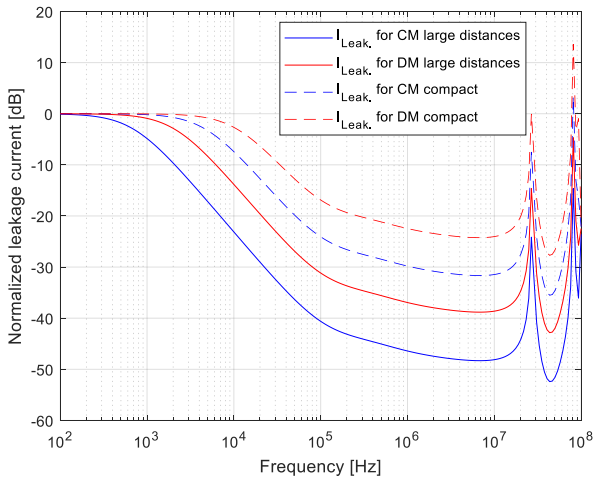


Fig. 8. Leakage current for CM and DM excitation for different distances between the cables and the cables to ground.

The higher the shield current, the lower the magnetic fields will be. It can be seen that larger distances reduce the cut-off frequency for CM and DM excitation. As small differences between excitation and shield currents can be responsible for major problems, the leakage current was calculated and is shown in Fig. 8. A small leakage current is preferred. The lowest leakage currents can be expected from the large cable distance configuration. The highest leakage current has to be expected from the compact configuration driven in differential mode. In the AM frequency range (500 kHz - 1.7 MHz) only a little bit more

attenuation than 20 dB has to be expected for the magnetic field. As space is limited in EV the compact parameter set is much more likely to be applied.

C. Analysis of External Voltage Drop

Equation (14) can give the external voltage drop along the shield, when the transfer impedance is given. In Fig. 9 it can be seen that due to similar currents starting from 100 kHz the longitudinal E-field is more or less independent from the geometry.

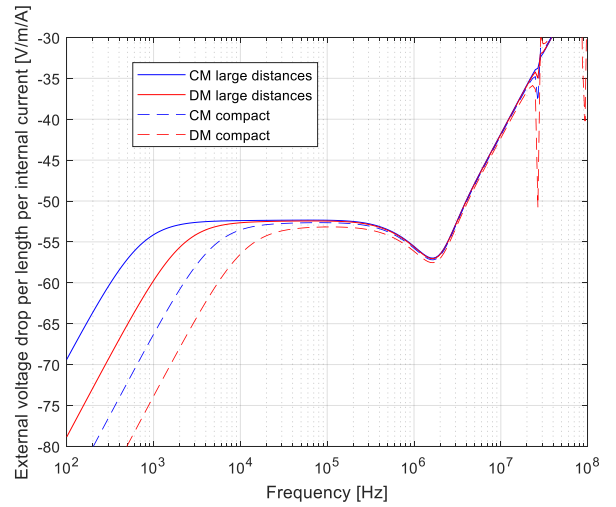


Fig. 9. External voltage drop for CM and DM excitation for different distances between the cables and the cables to ground.

D. Influence of connectors

As connectors can significantly affect the behavior of a shielded cable configuration two assumed connector impedances were investigated.

1. $Z_{Con}=1 \text{ m}\Omega+j\omega 2 \text{ nH}$, referred as “small”
2. $Z_{Con}=10 \text{ m}\Omega+j\omega 20 \text{ nH}$, referred as “large”

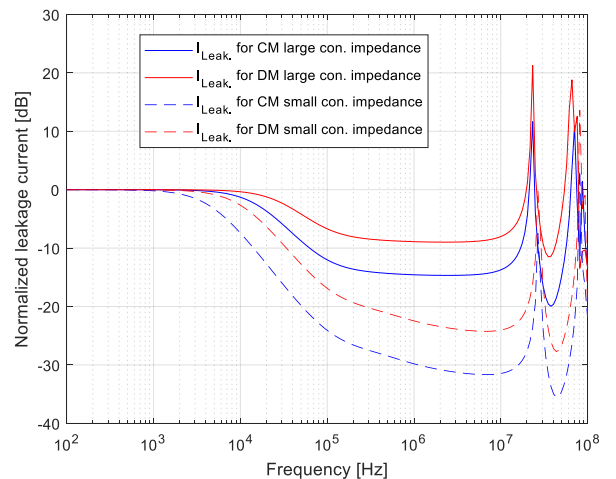


Fig. 10. Leakage current for CM and DM excitation for different connector impedances, large: $10 \text{ m}\Omega+j\omega 20 \text{ nH}$, small: $1 \text{ m}\Omega+j\omega 2 \text{ nH}$

In Fig. 10, the normalized leakage currents are shown for the “compact” geometry for the two presented connector impedances. It can be seen that an increase of the impedance by a factor of 10 leads in the medium frequency range to a rise of the leakage current by approximately 10 dB.

V. OPTIMIZING CABLE CONNECTOR SYSTEMS

The analytical method can be used to optimize cable and connector systems. In order to reduce weight, thin shield approaches are very interesting. When the thickness of the shield is reduced by a factor of 10 the cut-off frequency will rise. As shown in Fig. 11, with a thinner shield the leakage current needs higher frequencies to become low. Starting from 2 MHz there are nearly no differences any more between “normal” and the reduced shield.

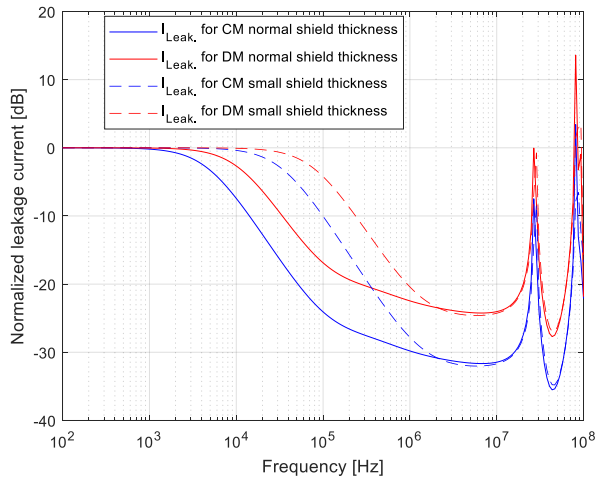


Fig. 11. Leakage current for CM and DM excitation for different shield thicknesses, normal: 200 μm , small: 20 μm

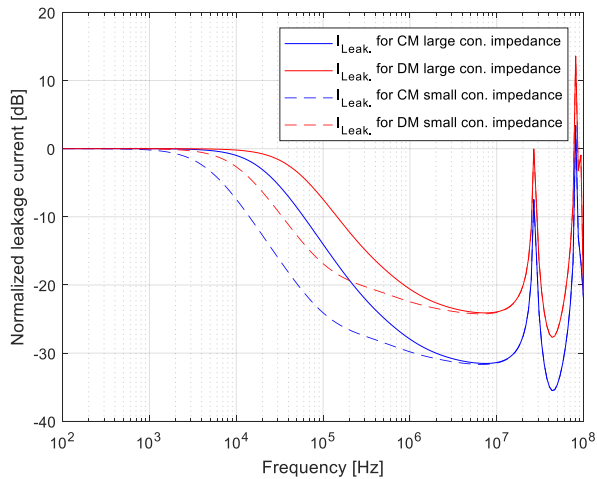


Fig. 12. Leakage current for CM and DM excitation for different connector impedances, large: 10 $\text{m}\Omega + j\omega$ 2 nH, small: 1 $\text{m}\Omega + j\omega$ 2 nH

Furthermore, the contact resistance of the connectors is often assumed to be an important system property. In Fig. 12, the leakage currents for two different contact resistance values are shown. Only in the frequency range between 1 kHz and 1 MHz

the contact resistance influence can be clearly seen. This means, neither the low frequency nor the higher frequency emission problems can be solved with lowering the contact resistance below 10 m Ω . A low leakage inductance is important.

VI. CONCLUSION

This paper has presented an analysis method for EV cable-connector systems based on MTL-theory. A configuration with two shielded cables, driven in DM- and CM-mode, was investigated. The leakage current, i.e. the current difference between the inner conductor and the shield, that is not compensated, was considered to be the most significant parameter. This current will dominate the external fields. The normalized leakage current can be used as a value for the shielding attenuation. Computations have shown that with realistic configurations attenuations of more than 30 dB are difficult to reach without additional special measures.

The presented analysis method can be an important step towards a better understanding of EV cable-connector systems and can be extended to three phase systems and more complex connector models using additional/different chain parameter matrices. EV cable-connector systems can be optimized with the given approach.

REFERENCES.

- [1] International Standard, *CISPR 25 - Vehicles, boats and internal combustion engines - Radio disturbance characteristics - Limits and methods of measurement for the protection of on-board receivers. ed. 4*, 2016.
- [2] International Commission on Non-Ionizing Radiation Protection, (ICNIRP), "Guidelines for Limiting Exposure to Time-Varying Electric and Magnetic Fields (1 Hz - 100 kHz)," *Health Physics* 99(6), 2010.
- [3] M. Reuter, S. Tenbohlen and W. Köhler, "The Influence of Network Impedance on Conducted Disturbances Within the High-Voltage Traction Harness of Electric Vehicles," *IEEE Transactions on EMC*, 2014.
- [4] A. Beltramelli, F. Grassi, G. Spadacini and S. A. Pignari, "Modeling Conducted Noise Propagation Along High-Voltage DC Power Buses for Electric Vehicle Applications," *International Conference on Connected Vehicles and Expo (ICCVE)*, 2014.
- [5] S. A. Schelkunoff, "The electromagnetic theory of coaxial transmission lines and cylindrical shields," *Bell Labs Technical Journal*, p. 532-579, 1934.
- [6] R. J. Mohr, "Coupling Between Open and Shielded Wire Lines Over a Ground Plane," *IEEE Transactions on EMC*, pp. 34-45, 1967.
- [7] C. R. Paul, "Application of multiconductor transmission line theory to the prediction of cable coupling," Tech. Rep. RADC-TR-76-101," Rome Air Development Center, 1980.
- [8] C. R. Paul, "Transmission-Line Modeling of Shielded Wires for Crosstalk Prediction," *IEEE Transactions on EMC*, 1981.
- [9] J. Meng, Y. X. Teo, D. W. P. Thomas and C. Christopoulos, "Fast Prediction of Transmission Line Radiated Emissions Using the Hertzian Dipole Method and Line-End Discontinuity Models," *IEEE Transactions on EMC*, 2014.
- [10] J. Rotgerink, G. Lansink and H. Schippers, "Generic prediction of crosstalk between shielded wires," *IEEE int. EMC Symposium*, 2015.
- [11] T. Sato, Y. Hayashi, T. Mizuki and H. Sone, "Simulation-based Analysis of Inductance at Loose Connector Contact Boundaries," *27th International Conference on Electrical Contacts*, 2014.
- [12] C. R. Paul, *Analysis of Multiconductor Transmission Lines*, Wiley, 1994.